P2.25

CONVECTIVE STORM INITIATION IN WESTERN CATALONIA: CHARACTERISTICS AND UNCERTAINTIES OF THE METHODOLOGY USED

Ramón Pascual

Instituto Nacional de Meteorología, Barcelona, Spain

INTRODUCTION

Forecasting of convection initiation is one of the main current challenges in operational tasks in the Spanish National Weather Service (INM). Knowledge of areas where convection develops most frequently is a previous step to obtain accurate nowcasts.

Regions of convective initiation can be identified from radar data using different methods, for example, identifying and tracking the potentially convective cells with and operational automated algorithm. This method was used previously to analyze 27 hailstorms occurred over western Catalonia between April and October, from 2000 to 2003. Now, a further careful subjective analysis has been made to discriminate the radar-detected storm initiation locations associated to meteorological phenomena from those related with the observational method itself and the characteristics of the algorithms used.

Different artifacts has appeared when examining the image loops: false splitting, old cells rebirth, ground clutter echoes intensification and alternation in characterization of a storm as a single cell or a multicell storm. These artifacts could be considered as part of a general problem of tracking complex visual objects from the radar point of view. It is necessary to extract these artifacts from the total set of storm initiation locations before to characterize storm initiation in this area.

DATA

Radar data: Table 1 summarizes the principal characteristics of the radar used.

- Lowest elevation scan: 0.5°. Height of the radar beam over study area: 1.5 km to 5 km.
- Orographic beam blockage: Important in a central band (Fig. 3).
- Ground clutter echoes: Study area almost free (Fig. 4) as corresponds to a low altitude flat area. Some echoes in the southeastern corner.
- Previous corrections: Ground clutter, orography screening effects, electronic fluctuations, and general signal decay due to rain over the radome (Sempere-Torres *et al.* 2003).
- Observing limitations: Path attenuation by rain and ground clutter echoes associated to anaprop conditions remain in corrected reflectivity fields.

Hail data belonging to the *Agrupació de Defensa Vegetal de les Terres de Ponent* have been used to select 27 episodes. The network, located in the plains of western Catalonia, covers an area of 3400 km2 and is inside the rectangle defined below. A set of 3888 polar volumes of radar reflectivity is available, 751 containing relevant information.

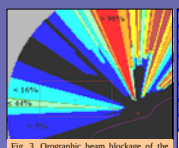

Fig. 3. Orographic beam blockage of the INM-Catalonia radar first elevation. Occultation is in %. The rectangle defines the study area. Adapted from INM.

Band (cm)	C: λ = 5.4
Resolution (km)	Normal: 2 x 2. Doppler: 1 x 1
Range (km)	Normal: 240. Doppler: 120
Exploration interval (min.)	10 both modes
Peak Power (kW)	250
Beamwidth (deg.)	0.9°
Pulselength (m)	Normal: 600. Doppler: 150

Table 1: Main characteristics of National Meteorological Institute (INM) radar at Catalonia.

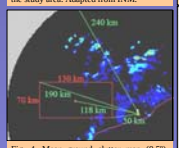

Fig. 4. Mean ground clutter map (0.5°). Darker blue corresponds to ground clutter from 0 km to 2.5 km. Rectangle (study area) dimensions (red) and distances (green). Adapted from INM.

Radar INM in Catalonia: 654 m M.S.L., 20 km south-west from Barcelona city. Photo: INM

Complementary data:

- Satellite imagery: **Characterization of convective structures, identification of convective cells and supporting of the synoptic and mesoscale diagnostic.**
- Numerical model outputs: **(INM-HIRLAM 0.5°) and sea level pressure/frontal analysis charts (Met. Office). Synoptic and mesoscale environment. Boundary layer convergence zones analysis.**
- Zaragoza INM sounding data (130 km westward the studied area): **Instability.**

Fig. 1. Catalonia situation at western Europe.

Fig. 2. Orographic map of Catalonia and surrounding areas indicating main features.

CONVECTIVE CELLS ORIGIN IDENTIFICATION

Identification, tracking and extrapolation software (YRADAR) based on the identification algorithm developed by Steiner *et al.* (1995), is operational on the INM-Mcldas system (Martín 2001).

This nowcasting tool has been ran over the selected first PPI in Cartesian coordinates generating a set of files that contain information about all the 2D potentially convective structures identified, henceforth named convective cells or cells (CEL0). Tracking allowed defining a cell as new when it is not linked to any previous structure (Wilson *et al.* 1986).

YRADAR has been developed to identify, characterize, track and extrapolate the more significant cells or mature cells present at time *t* in the radar domain. Therefore, it would not expect that can identify the first echo associated. However, further subjective analysis carried out has shown that the error in considering 2D new structures centroid coordinates and time to analyze convection initiation is small enough to accept the results presented here as a good first approximation.

YRADAR considers that a pixel is convective if: Z ≥ 45 dBZ or Z ≥ 40 dBZ and is a local maximum or the pixel is close enough to a convective pixel. YRADAR considers 4-connectivity to build 2D convective cells. Any restriction has been applied to convective cell dimension although for tracking purposes they have been classified as small (< 24 km2) and large (≥ 24 km2). Tracking method assigns large cells at instant *t* to the nearest large cells at instant *t-10'*. Small cells have been ever considered as new cells (Martín 2001).

RESULTS AND DISCUSSION

279 CEL0 have been identified (Fig. 5). Afterwards, a subjective detailed analysis have been carried out, building schematics as shown in Fig. 6, that can be simple or very complex depending on the episode duration, the triggering mechanisms, the number of new cells developed and the frequency and kind of interactions between them.

Fig. 5. Storm initiation locations. Blue dots: artifacts. Red dots: Meteorological cells. Notice the mountains in the southeastern corner of the study area.

Fig. 6. Example showing the evolution of the automated identified and tracked potentially convective cells observed during the 8 July 2002, between 19:20 UTC and 23:50 UTC. Black numbers: Number of old convective cell. Red numbers: New cells. Yellow numbers: Initiation times. Merges and splits are also indicated. Cov: Triggering in convergence lines. Out: Gust front triggering.

Examination of the loops has shown a set of artifacts considered new convective cells. 196 (70 %) cells have been considered meteorological new cells (CEL0M), 26 of them because of splitting, and 83 artifacts (30 %). Examples of artifacts are:

- **2D radar structures resulting from false splitting. False splitting may appear from breakage of a structure as a consequence of orographic beam blockage or path attenuation.**
- **Old cell rebirth. Sometimes, a structure can lose the convective category either as a consequence of internal real changes or because observational difficulties. Anyhow, cells appeared again would not be considered new cells. In Fig. 7 convective cell labeled 10 vanishes at 13:10 UTC appearing again 10 minutes later with label 5.**
- **Single cell-multicell alternation. 2D radar structures analysis frequently considers multicell storms as single cell storms with a unique centroid. Sometimes, during multicell storm motion and evolution "convective bridges" between local reflectivity maxima break losing contiguity in reflectivity field.**
- **Ground clutter echoes intensification under anaprop conditions. This echoes are very difficult to eliminate and therefore have been considered new convective cells.**
- **Incorrect tracking due to lack of wind data or extreme clustering. In this study wind data has not been used to assign radar structures in time *t* to structures in *t-10'*, and as a consequence, in a few cases assignation has been incorrect. Clustering also introduces uncertainty in tracking processes (Howard *et al.* 1997) and also suggests the presence of local or mesoscale triggering mechanisms, probably associated to PBL convergence zones (Wilson and Schreiber 1986; Koch and Ray 1997).**

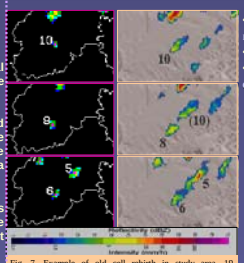

Fig. 7. Example of old cell rebirth in study area. 19 September 2000. Top: 13:00 UTC. Centre: 13:10 UTC. Bottom: 13:20 UTC. Left: Convective images obtained from YRADAR. Right: Reflectivity images obtained from VISRAD. First PPI.

- **A 50 % of the artifacts (CEL0F) have a lifetime of 10 ' while only a 37 % of CEL0M do it. This result shows a slightly more ephemeral nature of the artifacts.**
- **Artifacts have a significant tendency to develop very near of previous cells (Fig. 8).**
- **Clustering of new convective cells responds to mesoscale environment and convective scale dynamics but it is also associated to the presence of the artifacts (Fig. 9).**

- **D0min(class 2) and D1min(2) are significantly lesser than D0min(0,1) and D1min(0,1).**
- **D1min(0) is significantly lesser than D1min(1).**
- **90% of D0 and D1 are lesser than 215 km (the half of maximum possible distance).**
- **90% of D0min is lesser than 60 km, a 50% lesser than 30 km and a 25% lesser than 15 km.**
- **90% of D1min(0) is lesser than 40 km.**
- Spatial distribution of CEL0F shows a greater dispersion than that of CEL0M.
- CEL0F population is slightly displaced northeastward respect CEL0M population.
- CEL0M and CEL0F spatial density maximums are located at different places.

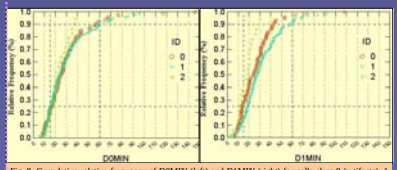

Fig. 8. Cumulative relative frequency of D0MIN (left) and D1MIN (right) for cells class 0 (artifacts), 1 (meteorological new cells) and 2 (resulting from splitting) . D0: Distances between the new convective cells in the rectangular area and all the cells scattered over the complete radar domain at time *t*. D1: Distances between the new convective cells present at time *t* and all the cells present at time t-10'. D0min, D1min: Mean value of the D0 and D1 minimum distances respectively.

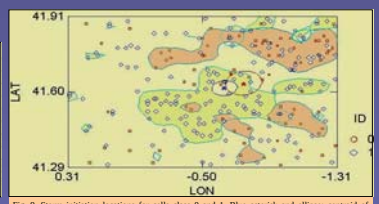

Fig. 9. Storm initiation locations for cells class 0 and 1. Blue asterisk and ellipse: centroid of meteorological cells population and confidence ellipse (p=0.95). Red asterisk and ellipse: centroid of artifacts population and confidence ellipse (p=0.95). Local maximums of concentrations have been showed applying a nonparametric kernel density estimator (p=0.150). Green and orange colored areas show these maximums.

New cells number (NCEL0T) daily distribution shows a great dispersion (min=0,max=28, mean=10.7, sd=7.1). Filtered database (NCEL0M) (min=0, max=22, mean=7.5, sd=5.3), shows less dispersion but still a long tail associated to 3 episodes (included between the five longest) (Fig. 10). Pearson coefficient between NCEL0M and duration is 0.852, showing a quasi-lineal dependence, better defined for values greater than 4 hours.

Correlation values between NCEL0T and NCEL0F and between NCEL0F and duration suggest dependence with factors that introduce non linearity: absolute and relative location and motion of convective cells over the radar domain (Fig. 11 and Fig. 12).

LI, TT and K indices (00 and 12 UTC soundings) have low correlation values with NCEL0M. Correlation has been calculated also between these indices and NCEL0M normalized by dividing by duration showing somewhat better values. TT seems to be the better correlated index (Fig. 13). CAPE and PW also show low correlations.

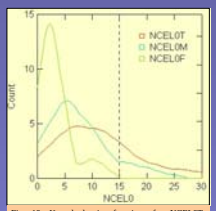

Fig. 10. Kernel density functions for NCEL0T, NCEL0M and NCELF. NCEL0= Number of new convective cells.

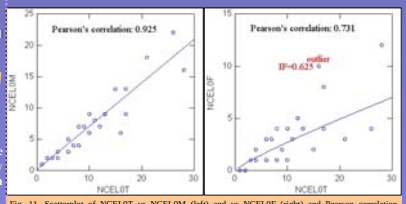

Fig. 11. Scatterplot of NCEL0T vs NCEL0M (left) and vs NCEL0F (right) and Pearson correlation coefficients. IF= NCEL0F/ NCEL0T. NCEL0F: Daily number of artifacts.

After filtering artifacts, an analysis of possible triggering mechanisms has been carried out. Splitting is a process that generates new convective cells but not a triggering mechanism. New cells have been classified as first or second generation convection regarding if they are associated or not to previous cells.

Two mechanisms have been considered here as responsible of secondary convection: gust front triggering and discrete propagation (Houze 2004). The analysis of location and motion relative between new and previous cells and the dimensions and evolution of convective structures has suggested that these mechanisms have reported for at least a 20% of cells class 1.

First generation convection is supposed to be linked to PBL convergence zones. Orography seems to be only relevant for the southeastern mountainous corner of the rectangular area.

Fig. 14 shows an example of convection initiation ahead a well defined eastward moving squall line. Cell 4 at 17:20 UTC probably develops in the interaction between a gust front or a gravity wave associated to the mesoscale system and a stationary convergence line apparent from small convective cells alignment.

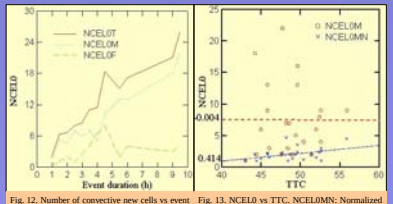

Fig. 12. Number of convective new cells vs event duration.

Fig. 13. NCEL0 vs TTC. NCEL0MN: Normalized NCEL0M. TTC: TT index extracted from the most recent sounding to convective episode onset.

Cell 4 (after 5) remains stationary over one of these lines and eventually merges with squall line (multicell 1).

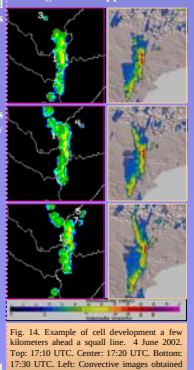

Fig. 14. Example of cell development a few kilometers ahead a squall line. 4 June 2002. Top: 17:10 UTC. Center: 17:20 UTC. Bottom: 17:30 UTC. Left: Convective images obtained from YRADAR. Right: Reflectivity images obtained from VISRAD. First PPI.

Finally a detailed subjective dynamical analysis has been made over the whole radar domain to identify the hypothetical convergence lines that could have affected study area. As in Pascual and Callado 2002, this analysis has been carried out in "precipitating" air, i.e., when precipitation is already detectable. To define these convergence/convective lines the next hypotheses have been applied:

- **Convective radar structures alignment must be supported by a convergence line.**
- **Convective cells distribution and relative motion between them have to be coherent with physical definition of convergence line.**
- **Convergence lines location, orientation and motion (absolute and relative between them) have to maintain an internal coherence and coherence with synoptic/mesoscale environment during the event.**

100 convergence/convective lines have been identified (Fig. 15), excluding gust fronts from this set. This analysis has shown that new convective cells develop mostly along these lines.

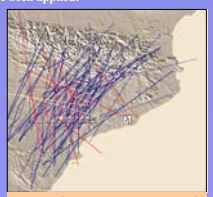

Fig. 15. Synthetic convective/convergence straight lines occurring during the selected 27 episodes. Different line colors/ styles used only for clarity. Black rectangle is the study area.

CONCLUSIONS

 # To obtain some radar-based general results about timing and location of convection initiation it is desirable to apply automated objective methods capable to carry out a correct identification and tracking of convective cells. Nevertheless, inherent features associated to observational method and algorithms characteristics restrict the validity of the results obtained.

 # 2D radar structures resulting from false splitting, old cell rebirth, single cell-multicell alternation, ground clutter echoes intensification and incorrect tracking due to lack of wind data or extreme clustering are the main factors that have created artifacts.

 # Distances between new convective and old cells shows that artifacts have a great tendency to be closer to old cells than meteorological ones. In addition, that artifacts have a more ephemeral nature. Some automated process that uses these artifacts qualities could be applied to filter a high number of them although some meteorological cells would be also removed.

 # Artifacts distribution shows a greater dispersion than meteorological new cells and its population is displaced northeastward, showing dependence with storm paths and may be with the relative beam blockage minimum north of maximum blockage band.

 # The poor correlation between the artifacts number and event duration suggests dependence with more complex factors that introduce non-linearity: absolute location and motion of convective cells over the radar domain and relative between them.

 # Convective activity depends primarily of factors like the triggering mechanisms time-space characteristics and their effectiveness. Secondary convection has had an important role in generating new convection due probably to the flat character of the study area and to the notable number of great convective structures and MCS.

 # Convective cells time-space distribution and motion has lead to conclude that they appear organized in straight lines which dimensions and evolution is coherent with synoptic/mesoscale environment. These lines have been considered convergence lines in order to account of the high proportion of new meteorological convective cells appeared over there.

REFERENCES

Houze, R. A., Jr., 2004: Mesoscale convective systems. *Rev. Geophys.*, 42, 0.1029/2004RG000150, 43 pp.

Howard, K. W., J. J. Gourley and R. A. Maddox, 1997: Uncertainties in WSR-88D measurements and their impacts on monitoring life cycles. *Weather and Forecasting*, 12, 166-174.

Koch, S. E. and C. A. Ray, 1997: Mesoanalysis of summertime convergence zones in central and eastern North Carolina. *Weather and Forecasting*, 12, 56-77.

Martín, F. 2001: Identificación objetiva de estructuras convectivas a partir de los datos radar del PPI/CAPPI bajo en MCIDAS. V Simposio Nacional de Predicción. INM.Madrid (Spain), 20-23 November 2001.

Pascual, R. and A. Callado, 2002. Mesoanalysis of recurrent convergence zones in north-eastern Iberian Peninsula. Preprints, *2nd European Conference on Radar Meteorology*, Delft, The Netherdlands, ERAD, 59-64.

Sempere-Torres, D.; Sanchez-Diezma, R.; Berenguer, M.; Pascual, R.; Zawadzki, I. 2003: Improving radar rainfall measurement stability using mountain returns in real time. 31th Conference on Radar Meteorology. Seattle (USA), 6-12 August 2003.

Steiner, M.; Houze, R. A.; Yuter, S. E. 1995: Climatological characterization of three dimensional storm structure from operational radar and raingauge data. *JAM*, 34, 1978-2007.

Wilson, J.W. and W. E. Schreiber, 1986: Initiation of convective storms at radar-observed boundary-layer convergence lines. *Monthly Weather Review*, 114, 2516-2536.